

# Effects of microstructure on the microwave dielectric properties of $\text{Ba}(\text{Co}_{1/3}\text{Nb}_{2/3})\text{O}_3$ and $(1-x)\text{Ba}(\text{Co}_{1/3}\text{Nb}_{2/3})\text{O}_3-x\text{Ba}(\text{Zn}_{1/3}\text{Nb}_{2/3})\text{O}_3$ ceramics

Cheol-Woo Ahn<sup>a</sup>, Hyun-Jung Jang<sup>a</sup>, Sahn Nahm<sup>a,\*</sup>, Hyun-Min Park<sup>b</sup>, Hwack-Joo Lee<sup>b</sup>

<sup>a</sup>Department of Materials Science and Engineering, Korea University, 1-5 Ka, Anam-Dong, Sungbuk-Ku, Seoul 136-701, South Korea

<sup>b</sup>New Materials Evaluation Center, Korea Research Institute of Standards and Science, Taeduk Science Town, Taejeon 305-600, South Korea

## Abstract

$\text{Ba}(\text{Co}_{1/3}\text{Nb}_{2/3})\text{O}_3$  (BCN) has a 1:2 ordered hexagonal structure. A large amount of the liquid phase, which contains high concentrations of Ba and Nb ions was found in the BCN ceramics.  $Q$ -values of BCN increased with increasing sintering temperature; however, it significantly decreased when the sintering temperature exceeded 1400 °C. The presence of a large amount of liquid phase could be responsible for the decrease of the  $Q$ -value. For  $(1-x)\text{Ba}(\text{Co}_{1/3}\text{Nb}_{2/3})\text{O}_3-x\text{Ba}(\text{Zn}_{1/3}\text{Nb}_{2/3})\text{O}_3$  [(1- $x$ )BCN- $x$ BZN] ceramics, the 1:2 ordered hexagonal structure was observed in the specimens with  $x \leq 0.3$  and the  $\text{BaNb}_6\text{O}_{16}$  second phase was found in the specimens with  $x \geq 0.6$ . Grain growth, which is related to the  $\text{BaNb}_6\text{O}_{16}$  second phase occurred in the specimens with  $x \geq 0.5$ . In this work, the excellent microwave dielectric properties of  $\tau_f = 0.0$  ppm/°C,  $\epsilon_r = 34.5$  and  $Q \times f = 97,000$  GHz were obtained for the 0.7BCN-0.3BZN ceramics sintered at 1400 °C for 20 h.

© 2003 Elsevier Ltd. All rights reserved.

**Keywords:** Dielectric properties; Microstructure-final; Niobates; Perovskite; Sintering

## 1. Introduction

Recently, investigations on the  $\text{Nb}_2\text{O}_5$  based complex perovskite ceramics has been increased to replace the expensive Ta-based complex perovskite ceramics for the application of microwave devices.<sup>1–3</sup> However, since the complicated microstructures such as liquid phase and grain growth usually develop in the  $\text{Nb}_2\text{O}_5$ -based complex ceramics, the understanding of both the structural variation and its effects on the microwave dielectric properties is necessary to obtain the required microwave dielectric properties. In the case of  $\text{Ba}(\text{Zn}_{1/3}\text{Nb}_{2/3})\text{O}_3$  (BZN) and  $\text{Ba}(\text{Ni}_{1/3}\text{Nb}_{2/3})\text{O}_3$  (BNN) ceramics, many investigations carried out on the structural variation and its effect on the microwave dielectric properties.<sup>2–4</sup> However, the microstructure of the BCN ceramic has not been clearly understood.

According to the previous works, BZN and BNN ceramics have the negative  $\tau_f$  and BCN has the positive  $\tau_f$  therefore, the (1- $x$ )BCN- $x$ BNN and (1- $x$ )BCN- $x$ BZN solid solutions have been studied to obtain a new materials which has the zero  $\tau_f$ .<sup>5,6</sup> Especially, BZN has a

high dielectric constant and a high  $Q$ -value, the (1- $x$ )BCN- $x$ BZN solid solution was expected to have excellent microwave dielectric properties.<sup>5,7</sup> However, even though many investigations have been conducted on the (1- $x$ )BCN- $x$ BZN ceramics, the microstructure and microwave dielectric properties of the (1- $x$ )BCN- $x$ BZN ceramics have not been completely understood.<sup>8</sup> In this work, BCN and (1- $x$ )BCN- $x$ BZN ceramics were produced under various process conditions and the microstructure and the microwave dielectric properties were studied. Especially, the variation of  $Q$ -value was explained in terms of the structural changes.

## 2. Experimental procedure

Ceramics of the composition  $(1-x)\text{Ba}(\text{Co}_{1/3}\text{Nb}_{2/3})\text{O}_3-x\text{Ba}(\text{Zn}_{1/3}\text{Nb}_{2/3})\text{O}_3$  with  $0.0 \leq x \leq 0.9$  were prepared from the oxides of >99% purity by using conventional solid state synthesis. Oxide compounds of  $\text{BaCO}_3$ ,  $\text{CoO}$ ,  $\text{ZnO}$  and  $\text{Nb}_2\text{O}_5$  were mixed for 24 h in a nylon jar with zirconia balls and then dried and calcined at 1100–1200 °C for 4 h. After remilling, the powder was dried and pressed into discs and sintered at 1300–1550 °C. The sintered specimens were cooled inside the furnace.

\* Corresponding author. Fax: +82-2-928-3584.

E-mail address: snahm@korea.ac.kr (S. Nahm).

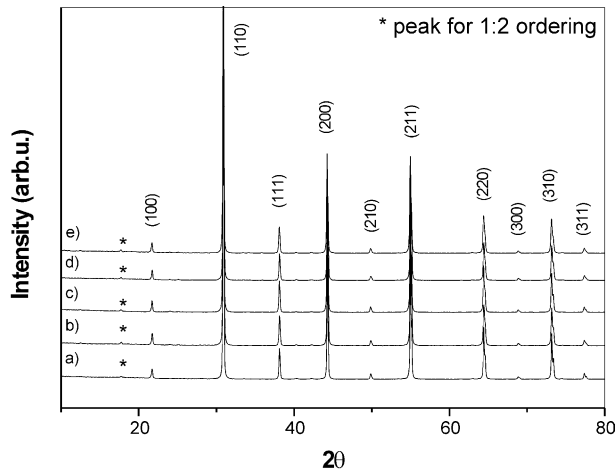


Fig. 1. XRD patterns of BCN ceramics sintered at: (a) 1350 °C, (b) 1400 °C, (c) 1450 °C, (d) 1480 °C and (e) 1550 °C for 6 h.

The cooling rate was about 20 °C/min until the temperature decreased to 800 °C, but it was difficult to measure the cooling rate below 800 °C. The microstructure of the specimen was studied by X-ray diffraction (XRD: Rigaku D/max-RC) and scanning electron microscopy (SEM: Hitachi S-4300). The densities of the sintered specimens were measured by water-immersion

technique. The dielectric properties were measured around 8.5–9.0 GHz at room temperature by a dielectric post resonator technique suggested by Hakki-Coleman<sup>9</sup> and Courtney.<sup>10</sup> The temperature coefficient of the resonant frequencies were measured at 6.5 GHz in the temperature range of 25 and 85 °C.

### 3. Results and discussion

#### 3.1. Microstructure and microwave dielectric properties of $Ba(Co_{1/3}Nb_{2/3})O_3$ ceramics

Fig. 1 shows X-ray diffraction patterns of BCN ceramics sintered at various temperatures for 6 h. All the peaks were indexed in terms of the 1:2 ordered hexagonal unit cell. The 1:2 ordering superlattice reflections indicated by asterisk were found in all diffraction patterns. Therefore, the 1:2 ordered hexagonal structure is developed in all the specimens. The peaks for the second phase were not observed.

Fig. 2(a)–(d) exhibit SEM images taken from both the thermally etched and the fracture surfaces of the BCN ceramics sintered at various temperatures for 6 h. The specimens sintered below 1400 °C have a homogeneous

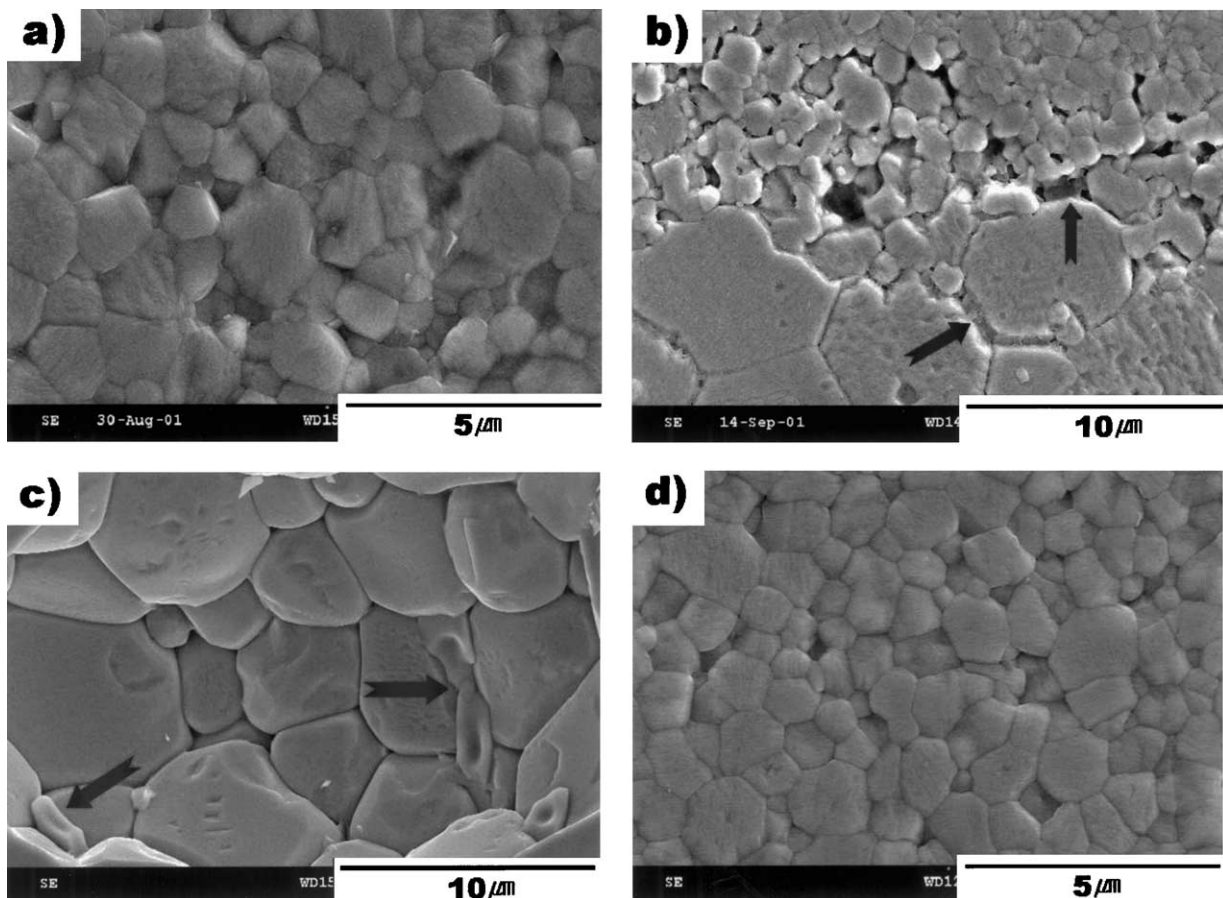


Fig. 2. SEM images of BCN ceramics sintered for 6 h at: (a) 1400 °C, (b) 1420 °C, (c) 1450 °C (fracture surface) and (d) 1450 °C (muffled with CoO).

Table 1  
Chemical compositions of the matrix and the liquid phase of  $\text{Ba}(\text{Co}_{1/3}\text{Nb}_{2/3})\text{O}_3$  ceramics sintered at 1450 °C for 6 h

Element	Matrix (at.%)	Liquid phase (at.%)
Ba	53.12	43.36
Co	18.47	9.34
Nb	28.41	47.30

microstructure and the average grain size was about 1.5  $\mu\text{m}$ . For the specimen sintered at 1420 °C, grain growth started and the size of some of the grains have already increased as shown in Fig. 2(b). For the specimens sintered at 1450 °C, the average grain was 10  $\mu\text{m}$ . A large amount of the liquid phase indicated by the arrow was found in the specimens sintered above 1400 °C [see Fig. 2(b) and (c)], the presence of the liquid phase is responsible for the grain growth. The composition of the liquid phase was investigated using energy dispersive spectroscopy (EDS) on the specimen shown in Fig. 2(c) and the results are illustrated in Table 1. The concentration of the Ba, Co, and Nb ions in the matrix are close to those of the nominal compositions. However, in the liquid phase, the concentrations of the Nb and Ba ions are high but that of Co ion is low. Therefore, the liquid phase is considered to be a Ba- and Nb-rich phase.

For  $\text{Ba}(\text{Zn}_{1/3}\text{Nb}_{2/3})\text{O}_3$  ceramics, the liquid phase containing high concentrations of Ba and Nb ions was also found and the formation of the liquid phase was explained by the evaporation of  $\text{ZnO}$ .<sup>3</sup> Since the evaporation of the  $\text{CoO}$  was also observed for the BCN ceramics sintered at high temperature, the formation of the liquid phase in BCN ceramics could be related to the

evaporation of  $\text{CoO}$ . In order to clarify the effect of the evaporation of  $\text{CoO}$ , BCN ceramics was sintered at 1450 °C with  $\text{CoO}$  muffling to prevent the evaporation of  $\text{CoO}$ . Neither the liquid phase nor grain growth was observed in this specimen as shown in Fig. 2(d). Therefore, it can be suggested that the evaporation of  $\text{CoO}$  contributes to the formation of the liquid phase in BCN ceramics.

Variations of the relative density, dielectric constant,  $\tau_f$  and  $Q \times f$  value with the sintering temperature are illustrated in Fig. 3. The relative density of the specimens slightly decreased when the sintering temperature exceeded 1400 °C but the decrease is not significant. The relative density of all the specimens was high above 95.5% of the theoretical density. The dielectric constant of the BCN sintered at 1350 °C was about 32.7 and the variation of the dielectric constant with the sintering temperature is not significant ranging between 32.5 and 33. The  $\tau_f$  of the specimen sintered at 1350 °C was about  $-10 \text{ ppm}/^\circ\text{C}$  and it increased when the sintering temperature exceeded 1400 °C at which the microstructure of the specimen significantly changed. Therefore, the variation of the microstructure is considered to affect  $\tau_f$  of the specimen but the details of the mechanism are not completely understood. Fig. 3 also shows the  $Q \times f$  value of the specimens sintered at various temperatures. The  $Q \times f$  value of the specimen sintered at 1350 °C was about 60,000 GHz and it increased with the sintering temperature showing the maximum value, 78,000 GHz, for the specimen sintered at 1400 °C. However, it suddenly decreased when the sintering temperature exceeded 1400 °C. The grain size increased with the sintering temperature and the relative density of all the specimens was high. Therefore, the deterioration of the  $Q$ -value cannot be explained by the variations of the grain size and the relative density. On the contrary, since a large amount of the liquid phase existed in the specimens sintered above 1400 °C, the decrease of the  $Q$ -value could be due to the presence of the liquid phase.

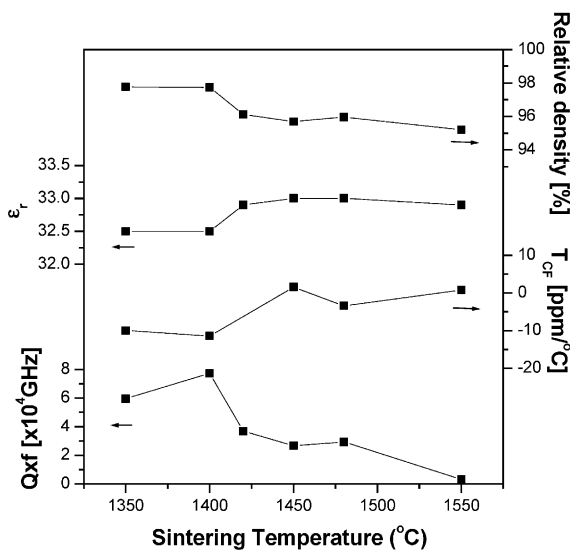


Fig. 3. Variations of the relative density, the dielectric constant, the temperature coefficient of the resonant frequency and  $Q \times f$  value of BCN ceramics sintered at various temperatures for 6 h.

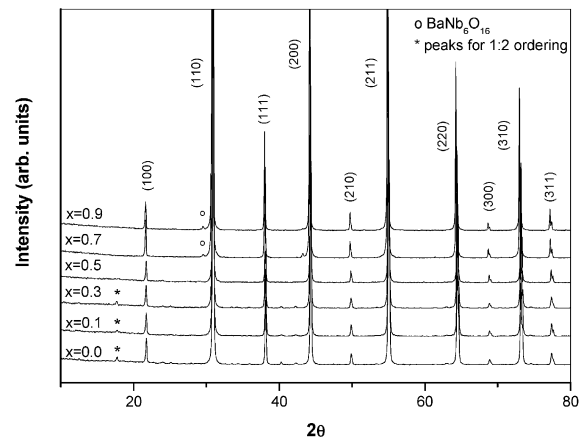


Fig. 4. X-ray diffraction patterns of the  $(1-x)\text{BCN}-x\text{BZN}$  ceramics with  $0.0 \leq x \leq 1.0$  sintered at 1400 °C for 6 h.

### 3.2. Microstructure and microwave dielectric properties of $(1-x)\text{Ba}(\text{Co}_{1/3}\text{Nb}_{2/3})\text{O}_3-x\text{Ba}(\text{Zn}_{1/3}\text{Nb}_{2/3})\text{O}_3$ ceramics

Fig. 4 shows the X-ray diffraction patterns of the  $(1-x)\text{Ba}(\text{Co}_{1/3}\text{Nb}_{2/3})\text{O}_3-x\text{Ba}(\text{Zn}_{1/3}\text{Nb}_{2/3})\text{O}_3$  ceramics with  $0.0 < x < 1.0$  sintered at  $1400\text{ }^\circ\text{C}$  for 6 h. The 1:2 ordering shown in the specimens with  $x \leq 0.3$  disappeared when  $x$  exceeded 0.3. According to the previous result, the 1:2 ordered structure which exists in BZN ceramics sintered at  $1300\text{ }^\circ\text{C}$ , disappeared in the BZN ceramics sintered at  $1400\text{ }^\circ\text{C}$  and it was explained by the evaporation of the ZnO.<sup>3</sup> Therefore, the disturbance of the 1:2 ordering occurred in the  $(1-x)\text{Ba}(\text{Co}_{1/3}\text{Nb}_{2/3})\text{O}_3-x\text{Ba}(\text{Zn}_{1/3}\text{Nb}_{2/3})\text{O}_3$  ceramics with  $x > 0.3$  can be attributed to the evaporation of the ZnO during the sintering. The XRD patterns show that the  $\text{BaNb}_6\text{O}_{16}$  second phase, which was found in BZN also exists in the specimens with  $x \geq 0.6$ . In addition, X-ray analysis also carried out on the 0.7BCN–0.3BZN specimens sintered at various temperatures and the 1:2 ordering disappeared for the specimens sintered above  $1400\text{ }^\circ\text{C}$ . Thus, the transition temperature of the 1:2 ordering for the 0.7BCN–0.3BZN specimens is between  $1400$  and  $1450\text{ }^\circ\text{C}$ .

Fig. 5(a)–(d) show the SEM images of the  $(1-x)\text{Ba}(\text{Co}_{1/3}\text{Nb}_{2/3})\text{O}_3-x\text{Ba}(\text{Zn}_{1/3}\text{Nb}_{2/3})\text{O}_3$  ceramics with  $0.0 < x < 1.0$  sintered at  $1400\text{ }^\circ\text{C}$  for 6 h. For the specimens with  $x \leq 0.3$ , the homogeneous microstructure without second phase was developed and the average grain size was about  $2.5\text{ }\mu\text{m}$ . The grains of the specimen started to grow when  $x = 0.5$  and for the specimen with  $x = 0.7$ , the grain growth was completed with the average grain size of  $10\text{ }\mu\text{m}$ . The grain growth occurred for the BZN ceramics sintered above  $1300\text{ }^\circ\text{C}$  and it is attributed to the presence of the  $\text{BaNb}_6\text{O}_{16}$  second phase whose melting temperature is about  $1320\text{ }^\circ\text{C}$ .<sup>3</sup> Therefore, the grain growth occurred in the specimens with  $x \geq 0.5$  also can be explained by the presence of the  $\text{BaNb}_6\text{O}_{16}$  second phase. From the XRD and SEM results, it can be suggested that the microstructure of the specimens with  $x \leq 0.3$  is very similar to that of BCN ceramics and for specimens with  $x \geq 0.5$ , the microstructure is similar to that of BZN ceramics.

Variations of the  $\tau_f$ , dielectric constant and  $Q \times f$  value of the specimens were illustrated in Fig. 6. The  $\tau_f$  linearly increased with the increasing  $x$  and it is close to zero when  $x = 0.3$ . The dielectric constant of the BCN is about 33 and that of BZN is 41. The dielectric constant

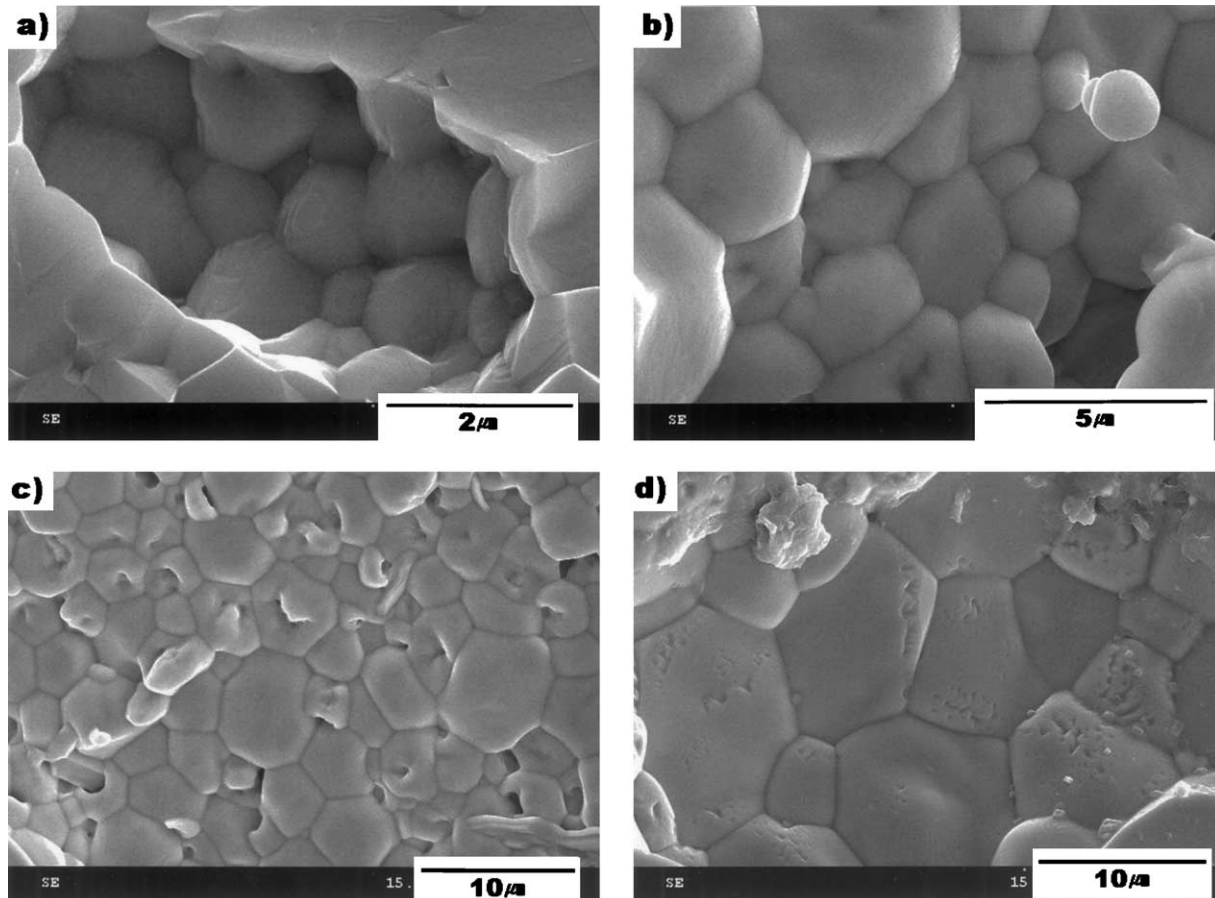


Fig. 5. SEM images of the  $(1-x)\text{BCN}-x\text{BZN}$  ceramics sintered at  $1400\text{ }^\circ\text{C}$  for 6 h: (a)  $x = 0.0$  (b)  $x = 0.3$ , (c)  $x = 0.5$  and (d)  $x = 0.7$ .

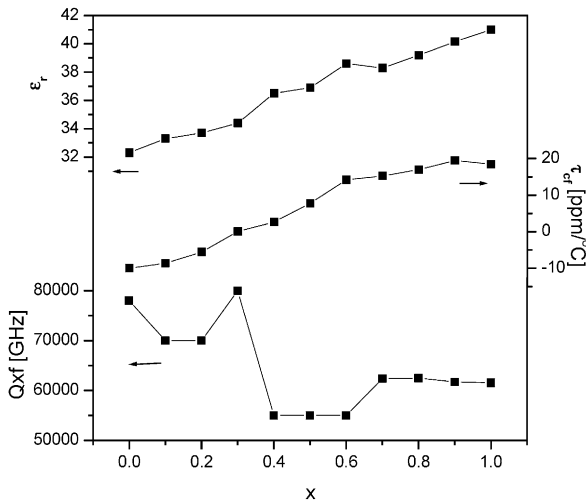


Fig. 6. Dielectric constant, temperature coefficient of the resonance frequency and  $Q \times f$  value for the  $(1-x)\text{BCN}-x\text{BZN}$  ceramics with  $0.0 \leq x \leq 1.0$  sintered at  $1400^\circ\text{C}$  for 6 h.

also linearly increased with the increase of  $x$  and it is about 34.5 for the 0.3BCN–0.7BZN ceramics, which has the zero  $\tau_f$ . The  $Q$ -value of the specimens can be divided into two parts. For the specimens with  $x \leq 0.3$ , the  $Q \times f$  value is high above 70,000 GHz, which is similar to that of BCN. On the contrary, for the specimens with  $x > 0.3$ , it is similar to BZN about 55,000 GHz. Since the microstructure of the specimens with  $x \leq 0.3$  is similar to that of BCN ceramics and for the specimens with  $x \geq 0.5$ , the microstructure is similar to that of BZN ceramics, it is considered that the  $Q$ -value of the  $(1-x)\text{Ba}(\text{Co}_{1/3}\text{Nb}_{2/3})\text{O}_3-x\text{Ba}(\text{Zn}_{1/3}\text{Nb}_{2/3})\text{O}_3$  ceramics is closely related to microstructure of the specimens.

According to the above results, the 0.7BCN–0.3BZN ceramics sintered at  $1400^\circ\text{C}$  has the excellent micro-

wave dielectric properties of  $\tau_f = 0$  ppm/°C,  $\epsilon_r = 34.5$  and  $Q \times f = 80,000$  GHz. Therefore, the detailed investigation was carried out on the 0.7BCN–0.3BZN ceramics. Fig. 7 illustrated the variations of the  $\epsilon_r$ , average grain size and  $Q$ -value of the 0.7BCN–0.3BZN sintered at  $1400^\circ\text{C}$  for various times. The variation of the  $\epsilon_r$  with the sintering time is negligible ranged between 34 and 35. The grain size of the specimens sintered for 2 h was about  $1.7 \mu\text{m}$  and it increased with the increase of the sintering time. Liquid phase or abnormal grain growth have not been observed in this system. The  $Q \times f$  value of the specimen increased with the increase of the sintering time and for the specimens sintered for 20 h, it was about 97,000 GHz. The variation of the  $Q$ -value with the sintering time is similar to that of the grain size therefore, the increase of the  $Q$ -value with the sintering time could be related to the increase of the grain size.

#### 4. Conclusions

$\text{Ba}(\text{Co}_{1/3}\text{Nb}_{2/3})\text{O}_3$  ceramics has the 1:2 ordered hexagonal structure. The liquid phase containing high concentrations of Ba and Nb ions was observed for the specimens sintered above  $1400^\circ\text{C}$ . Grain growth occurred for the specimens sintered above  $1400^\circ\text{C}$ , which is due to the presence of the liquid phase during the sintering. The  $Q$ -value increased with increasing sintering temperature and the maximum  $Q$ -value was obtained for the BCN sintered at  $1400^\circ\text{C}$ . For the BCN sintered above  $1400^\circ\text{C}$ , the  $Q$ -value significantly decreased and it might be due to the presence of a large amount of the liquid phase.

For the  $(1-x)\text{BCN}-x\text{BZN}$  ceramics, the 1:2 ordered hexagonal structure was observed in the specimens with  $x \leq 0.3$  and the  $\text{BaNb}_6\text{O}_{16}$  second phase was found in the specimens with  $x \geq 0.6$ . The grain growth, which is related to the  $\text{BaNb}_6\text{O}_{16}$  phase occurred in the specimens with  $x \geq 0.5$ . The  $\tau_f$  increased with  $x$  and the specimens with  $0.3 \leq x \leq 0.4$  have zero  $\tau_f$ . The  $Q$ -value was high for the specimens with  $x \leq 0.3$  but it decreased when  $x$  exceeded 0.3. The  $Q$ -value of the specimens was greatly affected by the microstructure. In this work, the excellent microwave dielectric properties of  $\tau_f = 0.0$  ppm/°C,  $\epsilon_r = 34.5$  and  $Q \times f = 97,000$  GHz were obtained for the 0.7BCN–0.3BZN ceramics sintered at  $1400^\circ\text{C}$  for 20 h.

#### Acknowledgements

This work was partially supported by the Ministry of Education of Korea and one of authors acknowledged that this work was financially supported by Korean Ministry of Science and Technology through NRL Project.

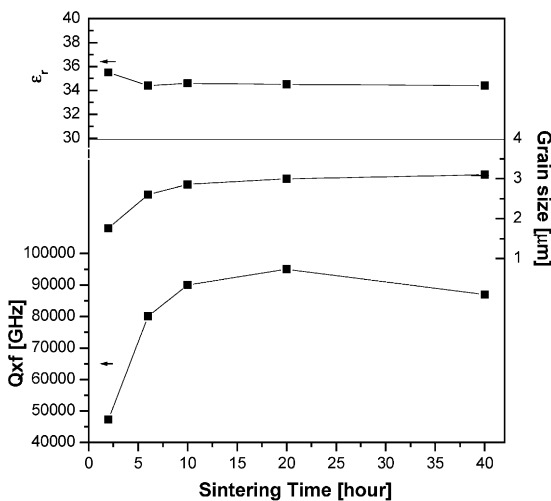


Fig. 7. Variations of the dielectric constant, the average grain size and the  $Q \times f$  value of the 0.7BCN–0.3BZN ceramics sintered at  $1400^\circ\text{C}$  for various times.

## References

1. Onoda, M., Kuwata, J., Kaneta, K., Toyama, K. and Nomura, S., Ba(Zn<sub>1/3</sub>Nb<sub>2/3</sub>)O<sub>3</sub>–Sr(Zn<sub>1/3</sub>Nb<sub>2/3</sub>)O<sub>3</sub> solid solution ceramics with temperature-stable high dielectric constant and low microwave loss. *Jpn. J. Appl. Phys.*, 1982, **21**, 1707–1710.
2. Hong, K. S., Kim, I. T. and Kim, C. D., Order–disorder phase formation in the complex perovskite compounds Ba(Ni<sub>1/3</sub>Nb<sub>2/3</sub>)O<sub>3</sub> and Ba(Zn<sub>1/3</sub>Nb<sub>2/3</sub>)O<sub>3</sub>. *J. Am. Ceram. Soc.*, 1996, **79**, 3218–3224.
3. Noh, S. Y., You, M. J., Nahm, S., Choi, C. H., Park, H. M. and Lee, H. J., Effect of structural changes on the microwave dielectric properties of Ba(Zn<sub>1/3</sub>Nb<sub>2/3</sub>)O<sub>3</sub> ceramics. *Jpn. J. Appl. Phys.*, 2002, **41**, 2978–2981.
4. Kim, I. T., Hong, K. S. and Yoon, S. J., Effects on non-stoichiometry and chemical inhomogeneity on the order–disorder phase formation in the complex perovskite compounds, Ba(Ni<sub>1/3</sub>Nb<sub>2/3</sub>)O<sub>3</sub> and Ba(Zn<sub>1/3</sub>Nb<sub>2/3</sub>)O<sub>3</sub>. *J. Mat. Sci.*, 1995, **30**, 514–521.
5. Sun, J. S., Yu, J. J., You, J. C. and Wei, C. C., Microwave dielectric properties of Ba(Sn<sub>x</sub>Zn<sub>(1-x)/3</sub>Nb<sub>(1-x)/3</sub>)O<sub>3</sub> (0 ≤ x ≤ 0.32) ceramics. *J. Mat. Sci.*, 1993, **28**, 2163–2168.
6. You, C. C., Huang, C. L., Wei, C. C. and Huang, J. W., Improved high-Q dielectric resonator sintered at low firing temperature. *Jpn. J. Appl. Phys.*, 1995, **34**, 1911–1915.
7. Kim, J. S., Lee, J. H., Lim, Y. S., Jang, J. W. and Kim, I. T., Revisit to the anomaly in dielectric properties of (Ba<sub>1-x</sub>Sr<sub>x</sub>)(Zn<sub>1/3</sub>Nb<sub>2/3</sub>)O<sub>3</sub> solid solution system. *Jpn. J. Appl. Phys.*, 1997, **36**, 5558–5561.
8. Endo, K., Fujimoto, K. and Murakawa, K., Dielectric properties of ceramics in Ba(Co<sub>1/3</sub>Nb<sub>2/3</sub>)O<sub>3-x</sub>Ba(Zn<sub>1/3</sub>Nb<sub>2/3</sub>)O<sub>3</sub> solid solutions. *J. Am. Ceram. Soc.*, 1987, **70**, C215–C218.
9. Hakki, B. W. and Coleman, P. D., Dielectric resonator method of measuring inductive capacities in the millimeter range. *IRE. Trans. Microwave Theory Tech.*, 1960, **8**, 402–410.
10. Courtney, W. E., Analysis and evaluation of a method of measuring the complex permittivity of microwave insulators. *IEEE Trans. Microwave Theory Tech.*, 1970, **MTT-18**, 476–485.